

## A Protein Engineering Approach Differentiates the Functional Importance of Carbohydrate Moieties of Interleukin-5 Receptor $\alpha$

Tetsuya Ishino,<sup>†,‡</sup> Nicoleta J. Economou,<sup>†</sup> Karyn McFadden,<sup>†</sup> Meirav Zaks-Zilberman,<sup>†</sup> Monika Jost,<sup>‡</sup> Sabine Baxter,<sup>†</sup> Mark R. Contarino,<sup>†</sup> Adrian E. Harrington,<sup>†</sup> Patrick J. Loll,<sup>†</sup> Gianfranco Pasut,<sup>§</sup> Sam Lievens,<sup>||</sup> Jan Tavernier,<sup>||</sup> and Irwin Chaiken<sup>\*,†</sup>

<sup>†</sup>Department of Biochemistry and Molecular Biology, Drexel University College of Medicine, 11102 New College Building, 245 North 15th Street, Philadelphia, Pennsylvania 19102, United States

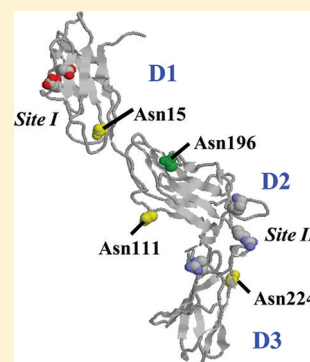
<sup>‡</sup>Department of Radiation Oncology, Drexel University College of Medicine, 11102 New College Building, 245 North 15th Street, Philadelphia, Pennsylvania 19102, United States

<sup>§</sup>Department of Pharmaceutical Sciences, University of Padua, Via F. Marzolo 5, Padua 35131, Italy

<sup>||</sup>Department of Medical Protein Research, Flanders Interuniversity Institute for Biotechnology, VIB09-Faculty of Medicine and Health Sciences, Ghent University, Ghent, Belgium

### **S** Supporting Information

**ABSTRACT:** Human interleukin-5 receptor  $\alpha$  (IL5R $\alpha$ ) is a glycoprotein that contains four N-glycosylation sites in the extracellular region. Previously, we found that enzymatic deglycosylation of IL5R $\alpha$  resulted in complete loss of IL5 binding. To localize the functionally important carbohydrate moieties, we employed site-directed mutagenesis at the N-glycosylation sites (Asn<sup>15</sup>, Asn<sup>111</sup>, Asn<sup>196</sup>, and Asn<sup>224</sup>). Because Asn-to-Gln mutagenesis caused a significant loss of structural integrity, we used diverse mutations to identify stability-preserving changes. We also rationally designed mutations at and around the N-glycosylation sites based on sequence alignment with mouse IL5R $\alpha$  and other cytokine receptors. These approaches were most successful at Asn<sup>15</sup>, Asn<sup>111</sup>, and Asn<sup>224</sup>. In contrast, any replacement at Asn<sup>196</sup> severely reduced stability, with the N196T mutant having a reduced binding affinity for IL5 and diminished biological activity because of the lack of cell surface expression. Lectin inhibition analysis suggested that the carbohydrate at Asn<sup>196</sup> is unlikely involved in direct ligand binding. Taking this into account, we constructed a stable variant, with triple mutational deglycosylation (N15D, I109V/V110T/N111D, and L223R/N224Q). The re-engineered protein retained Asn<sup>196</sup> while the other three glycosylation sites were eliminated. This mostly deglycosylated variant had the same ligand binding affinity and biological activity as fully glycosylated IL5R $\alpha$ , thus demonstrating a unique role for Asn<sup>196</sup> glycosylation in IL5R $\alpha$  function. The results suggest that unique carbohydrate groups in multiglycosylated receptors can be utilized asymmetrically for function.



Interleukin-5 (IL5) is a hematopoietic growth factor that promotes maturation, proliferation, and activation of eosinophils.<sup>1</sup> Although eosinophils play a major role in host defense by combating parasites, they are also central to tissue damage in several allergic disorders, including asthma and hypereosinophilic syndrome.<sup>2–4</sup> Hence, IL5 has been implicated in the pathogenesis of these inflammatory diseases.

IL5 exerts its effects through its cognate receptor on the cell surface of eosinophils. The IL5 receptor is composed of an  $\alpha$  subunit that binds IL5 specifically and a  $\beta$ c subunit that shares affinity for IL3 and GM-CSF and is responsible for cytoplasmic signal transduction. Data from cell FRET and other biochemical analyses suggest an activation model in which IL5 triggers cellular responses by sequentially binding first to IL5R $\alpha$  followed by binding of the complex to a preassembled  $\beta$ c subunit.<sup>5–8</sup>

We and others have investigated the structural elements underpinning molecular recognition in the complex between IL5 and IL5R $\alpha$  and have identified important characteristics of

epitope usage. The receptor binding elements in IL5 are dominated by charged residues in helix B (His<sup>38</sup>, Lys<sup>39</sup>, and His<sup>41</sup>), the C–D turn (Glu<sup>88</sup>, Glu<sup>89</sup>, Arg<sup>90</sup>, and Arg<sup>91</sup>), and helix D (Glu<sup>110</sup>).<sup>9,10</sup> For  $\beta$ c binding and signal transduction, Glu<sup>13</sup> in helix A is a key residue.<sup>10</sup> The ligand binding residues in IL5R $\alpha$  also are charged. These are located in domain 1 (Asp<sup>55</sup>, Asp<sup>56</sup>, and Glu<sup>58</sup>), domain 2 (Lys<sup>186</sup> and Arg<sup>188</sup>), and domain 3 (Arg<sup>297</sup>) of the three fibronectin-type III domains of the extracellular region of IL5R $\alpha$ .<sup>11,12</sup> A homology model of the IL5–IL5R $\alpha$  complex provided supporting evidence that a pair of complementary charged interfaces plays an important role in the specific interaction between IL5 and IL5R $\alpha$ .<sup>12</sup> Moreover, thermodynamic studies suggest that IL5R $\alpha$  is likely to undergo significant conformational rearrangement upon ligand binding, which might be important for  $\beta$ c recruitment and subsequent

**Received:** June 13, 2011

**Revised:** July 17, 2011

**Published:** July 19, 2011

receptor activation.<sup>13</sup> Such complementary charge–charge interactions and ensuing conformational rearrangement are likely the key steps in receptor activation.

While the biological function of a protein is primarily determined by its polypeptide sequence, glycosylation can have an impact on many aspects of its activity, such as intracellular trafficking, membrane secretion, folding, structure, stability, solubility, and interactions with binding partners.<sup>14–16</sup> IL5R $\alpha$  is a glycoprotein that contains four N-glycosylation sites (Asn<sup>15</sup>, Asn<sup>111</sup>, Asn<sup>196</sup>, and Asn<sup>224</sup>) in the extracellular region, and it was shown that ~14% of the total mass of the extracellular region of IL5R $\alpha$  is carbohydrate.<sup>13</sup> Previously, it was found that IL5R $\alpha$  deglycosylated by PNGase F could not bind to IL5, suggesting the importance of receptor glycosylation for stabilizing the structure of the receptor itself and/or receptor–ligand interaction.<sup>13</sup> However, it has remained unclear how glycosylation affects the ligand binding activity of IL5R $\alpha$  and whether individual glycosylation sites play a more important role than others. In this study, we investigated the functional roles of each of the four glycosylation sites in ligand binding activity, biological function, and cell surface expression of IL5R $\alpha$ . Because our initial trial of Asn-to-Gln mutagenesis caused a significant loss of stability judging from its binding to a conformationally sensitive antibody, we employed a more sophisticated protein engineering approach by combining apolar-to-polar mutations and homology-based mutagenesis.<sup>17,18</sup> This work led to a stable variant in which three of four glycosylation sites are eliminated (N15D, I109V/V110T/N111D, and L223R/N224Q). This mostly deglycosylated variant retained the same ligand binding affinity and biological activity as fully glycosylated IL5R $\alpha$ . We demonstrated in this work that protein engineering is a useful tool for identifying functionally critical glycosylation sites and deriving tools for structural analysis of other glycoproteins.

## EXPERIMENTAL PROCEDURES

**Materials.** Concanavalin A (ConA), bovine serum albumin (BSA), and mouse interleukin-3 (IL3) were purchased from Sigma-Aldrich (St. Louis, MO). Human interleukin-5 (IL5) and cyanovirin-N (CV-N) were produced and purified as previously described.<sup>19,20</sup> All the enzymes were purchased from New England Biolabs (Beverly, MA). All oligo DNA primers, *Drosophila* Schneider 2 (S2) cells, cell culture medium, L-glutamine solution, and RPMI 1640 medium were purchased from Invitrogen (Carlsbad, CA). The BaF3 cell line was purchased from German Collection of Microorganisms and Cell Cultures (DSMZ, Braunschweig, Germany). For surface plasmon resonance measurements (SPR), sensor chip CMS, surfactant P20, *N*-ethyl-*N*-[3-(dimethylamino)propyl]-carbodiimide (EDC), *N*-hydroxysuccinimide (NHS), 1 M ethanolamine (pH 8.5), and 10 mM glycine hydrochloride (glycine-HCl) (pH 1.5 and 2.0) were purchased from Biacore (Piscataway, NJ).

**S2 Cell Transient Expression of Soluble IL5R $\alpha$ .** For mutational deglycosylation of soluble IL5R $\alpha$ , site-directed mutagenesis was introduced into pMT-IL5R $\alpha$ -V5-His<sup>12</sup> using a QuikChange site-directed mutagenesis kit (Stratagene). The presence of the desired mutations was verified by DNA sequencing. *Drosophila* S2 cells were transiently transfected with vector pMT-IL5R $\alpha$ -V5-His together with pMT-GFP [expression vector for green fluorescent protein (Invitrogen)] using Cellfectin reagent (Invitrogen) and grown in serum-free

medium supplemented with 20 mM L-glutamine. Protein expression was induced by addition of 650  $\mu$ M copper sulfate 3 days after transfection. Cell-free supernatant was collected after 2 days and stored at  $-20$  °C for the following binding analysis.

**Protein Purification. Soluble IL5R $\alpha$ .** The soluble forms of human IL5R $\alpha$  and its deglycosylated variant with N15D, I109V/V110T/N111D, and L223R/N224Q mutations (denoted IL5R $\alpha$ [\DeltaN15/111/224]) were produced in stably transfected *Drosophila* S2 cells. The *Drosophila* expression vector and blasticidin-resistant vector pCoBlast (Invitrogen) were cotransfected into S2 cells using Cellfectin reagent (Invitrogen). Blasticidin-resistant cells were selected as a stable polyclonal population and grown in serum-free medium supplemented with 20 mM L-glutamine and 25  $\mu$ g/mL blasticidin S (Invitrogen). For expression, the cell density was expanded to approximately  $1 \times 10^7$  cells/mL and protein expression was induced by addition of 0.6 mM copper sulfate. The culture was harvested after 72 h and centrifuged at 1000g for 10 min. The soluble forms of IL5R $\alpha$  and the deglycosylated variant were purified as described previously.<sup>7</sup> Briefly, the cleared supernatant was loaded onto a 2B6R-conjugated affinity column, and bound proteins were eluted with 0.1 M glycine (pH 2.8). The resulting protein solution was neutralized with a 1 M Tris-HCl solution (pH 9.0), buffer exchanged to PBS, concentrated, and stored below  $-80$  °C. The ligand binding activity was confirmed by an SPR binding assay as described previously.<sup>12</sup>

**Anti-IL5R $\alpha$  Monoclonal Antibody.** 2B6R and  $\alpha$ 16 are mouse monoclonal antibodies raised against soluble IL5R $\alpha$ .<sup>7,21</sup> The hybridoma cells were maintained in RPMI 1640 medium with 10% FCS (Hyclone). Antibodies were purified by using protein G affinity column chromatography according to a standard procedure.

**Protein Characterization.** The purity of the protein was confirmed by Western blot analyses using polyacrylamide gel electrophoresis in the presence of 0.1% sodium dodecyl sulfate (SDS–PAGE). The integrity of proteins was verified by matrix-assisted laser desorption ionization mass spectrometry (MALDI-MS) (Wistar Institute, Philadelphia, PA). Protein quantitation was achieved by measuring the absorbance at 280 nm and calculating the concentration using the molar absorption coefficient using the method of Pace et al.<sup>22</sup>

**SPR Biosensor Binding Analysis.** The kinetic interaction assay was conducted using an SPR biosensor, Biacore 3000 (Biacore Inc., Uppsala, Sweden). All the experiments were conducted at 25 °C in PBS buffer containing 0.005% P20.

**Screening Assay for the Structural Integrity of IL5R $\alpha$  Deglycosylation Mutants.** We used four different antibodies, namely, 17b (anti-HIV gp120 mAb<sup>23</sup>), anti-GFP pAb (Clontech), anti-V5-tag pAb (Invitrogen), and  $\alpha$ 16 (anti-human IL5R $\alpha$  mAb<sup>21</sup>). For immobilization of the antibodies on a CMS sensor chip, a 1 mg/mL protein stock solution was diluted 50-fold in 10 mM acetate (pH 4.5) and injected onto a biosensor surface that had been preactivated with a 1:1 mixture of 200 mM EDC and 50 mM NHS, followed by the injection of 1 M ethanolamine hydrochloride (pH 8.5). Transiently expressed IL5R $\alpha$  mutational variants were injected over the antibody-immobilized surface. After the surface had been washed, the amount of bound protein was measured for each antibody surface. To regenerate chip surfaces, bound proteins

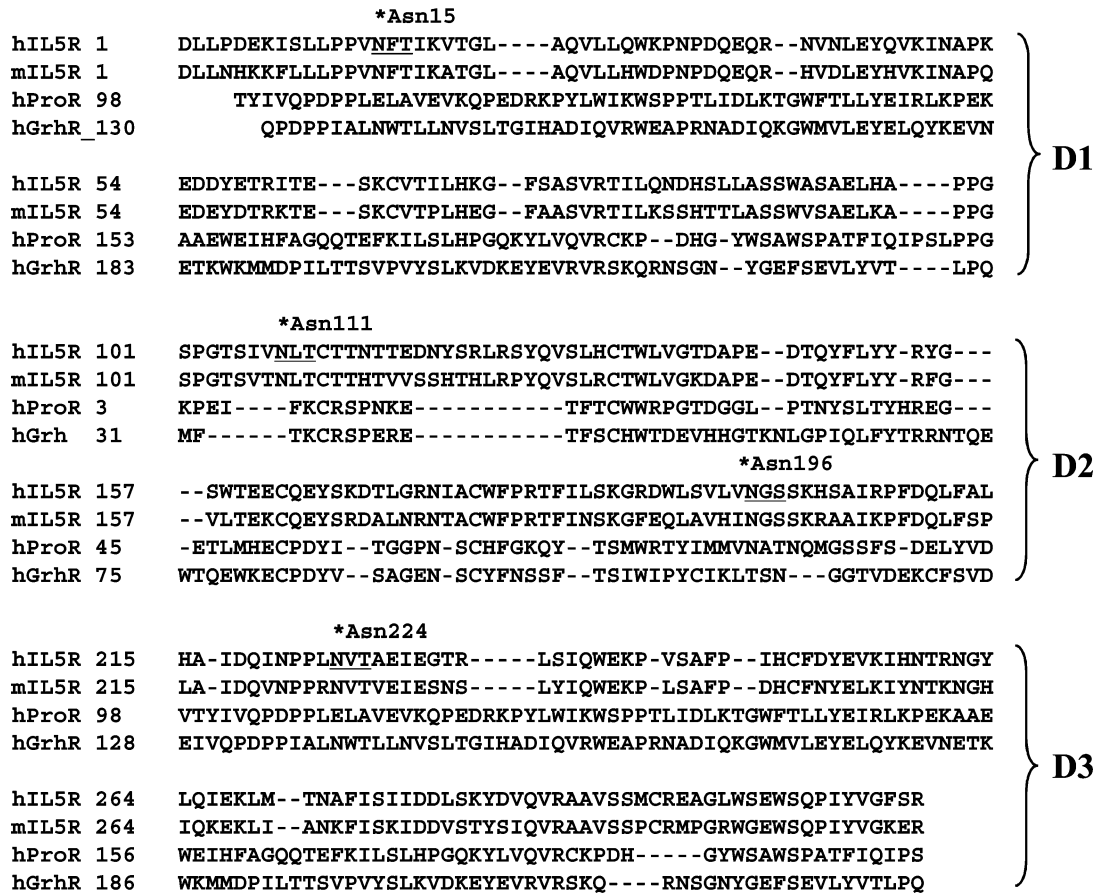


**Figure 1.** Sequence alignment of the extracellular domain of IL5R $\alpha$  and other cytokine receptors. Multiple-sequence alignments of human and mouse IL5R $\alpha$ , human prolactin receptor, and human growth hormone receptor were performed by using ClustalW version 1.60<sup>49</sup> and further adjusted manually. Three fibronectin type III domains of IL5R $\alpha$  are denoted D1, D2, and D3.

were removed from the antibody surfaces with 10 mM glycine-HCl (pH 1.6).

**Interaction between IL5 and IL5R $\alpha$  Deglycosylation Mutants.** To determine the binding affinity for IL5, we employed a previously established “on-chip purification” method,<sup>12</sup> in which culture medium containing the V5-tagged receptor protein was injected over an anti-V5 antibody surface. Analogous to affinity column chromatography, only the tagged receptor was precaptured on the chip surface, while all of the nonspecific components were washed away. Subsequently, various concentrations of IL5 were injected into the flow cell containing a particular precaptured IL5R $\alpha$  deglycosylated variant as well as a control surface. To regenerate the chip surfaces, both captured and bound proteins were removed from the antibody surfaces by double injections of a 10 mM glycine-HCl solution (pH 1.6). For this sensor assay, all procedures were automated to create repetitive cycles of injection of cell-free culture (10  $\mu$ L/min), 0–40 nM IL5 (50  $\mu$ L/min), and regeneration buffer (100  $\mu$ L/min). The injection time for the variants was varied to achieve a similar extent of capturing (approximately 200 RU). For the IL5R $\alpha$ [ $\Delta$ N196] variant, the binding assay was conducted with a higher-density receptor surface (up to 800 RU).

**Lectin Binding and Inhibition Assay.** Immobilization of lectins (ConA and CV-N) on a CMS sensor chip was conducted by the amine coupling method as described above. The real-time interaction was measured by injecting purified IL5R $\alpha$  or IL5R $\alpha$ [ $\Delta$ N15/111/224] onto these surfaces. Bound

proteins were removed from the surfaces by triple injections of 10 mM glycine-HCl (pH 1.6) after each cycle. All the procedures were automated to create repetitive cycles of injection of various concentrations of purified IL5R $\alpha$  or IL5R $\alpha$ [ $\Delta$ N15/111/224] (flow rate of 50  $\mu$ L/min), and regeneration buffer (flow rate of 100  $\mu$ L/min). To examine whether CV-N affects the IL5–IL5R $\alpha$ [ $\Delta$ N15/111/224] interaction, different concentrations of IL5 were passed over the IL5R $\alpha$ [ $\Delta$ N15/111/224] captured by CV-N or  $\alpha$ 16 (control).

**Data Analysis.** Nonlinear least-squares analysis was used to calculate the association and dissociation rate constants ( $k_{on}$  and  $k_{off}$ , respectively). Prior to the calculation, the binding data were corrected for nonspecific interaction by subtracting the reference surface data from the reaction surface data and further corrected for the buffer effect by subtracting the signal due to buffer injections from those of protein sample injections.<sup>24</sup> The interaction curves thus obtained were globally fit using a model for 1:1 Langmuir binding (BIAevaluation, Biacore). Individual kinetic parameters were obtained from at least three separate experiments. The equilibrium dissociation constant ( $K_d$ ) was calculated with the relationship  $K_d = k_{off}/k_{on}$ .

**Construction of BaF3 Cell Lines Expressing Full-Length IL5R $\alpha$ .** Mammalian expression vector pcDNA3.1 (Invitrogen) encoding full-length IL5R $\alpha$  was subcloned by using pSV-SPORT-IL5R $\alpha$ <sup>25</sup> as a template. For full-length IL5R $\alpha$ [ $\Delta$ N196] and full-length IL5R $\alpha$ [ $\Delta$ N15/111/224], mutations were introduced into the pcDNA for full-length IL5R $\alpha$

using QuikChange site-directed mutagenesis kit (Stratagene). The mouse pro B lymphocyte IL3-dependent cell line, BaF3, was maintained in RPMI 1640 medium with 10% FCS (Hyclone) supplemented with 10 nM mouse IL3. For transfection, cells ( $2 \times 10^6$ ) were washed with PBS buffer and then incubated in 0.8 mL of PBS buffer containing 50  $\mu$ g of DNA for 10 min at 4 °C. Electroporation was performed using Gene Pulser II (Bio-Rad) at 300 V and 975  $\mu$ F. Subsequently, the cells were allowed to recover from transfection in the IL3-supplemented growth medium. Selection was initiated 48 h after transfection in the IL3-supplemented growth medium containing 600  $\mu$ g/mL G418 (Invitrogen). After 8–10 days, healthy populations of cells were obtained and maintained.

**Cell Proliferation Assay.** The assay was conducted using BaF3 cells expressing full-length IL5R $\alpha$ . These cells were washed four times in RPMI 1640 medium with 10% FCS (Hyclone) to remove residual mouse IL3 from the culture medium. Plates with 96 wells were seeded with 5000 cells/well (50  $\mu$ L) and incubated for 48 h (37 °C and 5% CO<sub>2</sub>) in the presence of different concentrations of human IL5 (50  $\mu$ L). Following the 48 h incubation, 10  $\mu$ L of WST-1 {4-[3-(4-iodophenyl)-2-(4-nitrophenyl)]-2H-5-tetrazolol-1,3-benzene disulfonate (Roche Diagnostics)} was added to each well and incubated for 4 h (37 °C). The plate was then read using a microplate reader at an absorbance of 450 nm with a 650 nm reference. Individual values were obtained from three experiments, and the average values with the standard deviation were plotted using Excel (Microsoft). To obtain the ED<sub>50</sub> value, the average values were fitted to a sigmoidal dose–response model using Prism (GraphPad).

**Flow Cytometry.** For staining, cells were suspended in staining buffer (PBS with 10% BSA) and incubated with 20  $\mu$ g/mL  $\alpha$ 16 or 2B6R as the primary antibody or 17b as an isotype-matched control, for 30 min at 4 °C, followed by incubation with 20  $\mu$ g/mL Alexa Fluor 488-conjugated goat anti-mouse secondary antibody (Invitrogen) for 45 min at 4 °C. Cells were washed with staining buffer between antibody incubations. Flow cytometry analysis was performed using a FACSORT flow cytometer (BD Biosciences, San Diego, CA) with 488 nm excitation from an argon ion laser at 15 mW. The forward scatter threshold was set to exclude small debris. Alexa Fluor 488 log fluorescence was captured on the FL1 channel equipped with a 530 nm wavelength filter with a 30 nm bandwidth. Data were acquired using Lysis II (version 2.0, BD Biosciences). At least 10000 events were acquired per sample. Data analysis was performed using WinMDI (version 2.8, J. Trotter, Scripps Research Institute, La Jolla, CA, available at <http://www.facs.scripps.edu>).

**Homology Modeling.** The three-dimensional structure of IL5R $\alpha$ [ $\Delta$ N15/111/224] was modeled using MODELLER 6v2.<sup>26</sup> The previously reported modeled structure of wild-type IL5R $\alpha$ <sup>12</sup> was used as a template. Basic steric principles such as close contacts or violation of stereochemistry were examined using PROCHECK,<sup>27</sup> and the three-dimensional profiles of the models were examined using ProSAII.<sup>28</sup> On the basis of these quality checks, the best modeled structure was chosen.

## RESULTS

**Assessment of the Structural Integrity of IL5R $\alpha$ .** To define the functional roles of each N-linked carbohydrate moiety at Asn<sup>15</sup>, Asn<sup>111</sup>, Asn<sup>196</sup>, and Asn<sup>224</sup> of IL5R $\alpha$  (Figure

1), we performed site-directed mutagenesis at the N-glycosylation sites and investigated both the ligand binding activity and the structural integrity of the mutants. The extracellular region of IL5R $\alpha$  was fused with the V5-tag peptide at its C-terminus and was expressed in S2 cells as described previously.<sup>12</sup> Prior to functional analyses of deglycosylation mutants of IL5R $\alpha$ , we first tested whether the mutations could affect the structural integrity of IL5R $\alpha$ . We previously found that an anti-IL5R $\alpha$  mAb  $\alpha$ 16<sup>21</sup> recognizes a three-dimensional epitope of IL5R $\alpha$ .<sup>12</sup> In this study, we demonstrated that the soluble form of IL5R $\alpha$  protein denatured via SDS–PAGE was detected by anti-IL5R $\alpha$  mAb, 2B6R, and anti-V5-tag antibody while it was not detected by  $\alpha$ 16 (Figure 2A). These findings suggest that  $\alpha$ 16 is a conformationally sensitive antibody. We developed a high-throughput assay in which  $\alpha$ 16 was immobilized on a biosensor surface to examine the stability of transiently expressed proteins. The anti-V5-tag antibody was also immobilized onto a different biosensor chip surface to normalize the expression level of the protein. As a proof of concept, we demonstrated that heat-denatured purified IL5R $\alpha$  was bound to the anti-V5-tag antibody but failed to bind to  $\alpha$ 16 (Figure 2B), whereas native IL5R $\alpha$  was bound to both  $\alpha$ 16 and the anti-V5-tag antibody (Figure 2C). Thus, we employed this method to verify the structural integrity of various deglycosylated mutants of IL5R $\alpha$ .

**Design of Mutationally Deglycosylated IL5R $\alpha$  Variants.** We first used diverse mutations to identify conformation-preserving changes at Asn<sup>15</sup>, Asn<sup>111</sup>, Asn<sup>196</sup>, and Asn<sup>224</sup>, the four glycosylation sites in IL5R $\alpha$ . For replacement of asparagine, we chose four charged residues (aspartic acid, glutamic acid, lysine, and arginine), one neutral residue (glutamine), and one hydrophobic residue (valine), all of which have molecular volumes similar to that of asparagine. Deglycosylated mutants were transiently expressed and subjected to the structural integrity assay described above. The data are shown in Figure 3. Mutations such as N15D, N111D, and N224K displayed significantly increased stabilities relative to those of Asn-to-Gln mutations (Figure 3A). Of note, replacement with valine at any of the glycosylation sites largely reduced the level of  $\alpha$ 16 binding, indicating that the four N-glycosylation sites are exposed to the solvent, and thus, the hydrophobic residue introduced at these positions might destabilize the structure of IL5R $\alpha$ . Because replacement of Asn<sup>196</sup> with any of these six residues severely reduced stability, we expanded mutations of Asn<sup>196</sup> to all other amino acid residues except cysteine, which could cause dimerization of IL5R $\alpha$ . We found that the Asn-to-Thr mutation was the best among those replacements (Figure 3B).

Second, we designed several mutations on the basis of a hypothesis that apolar-to-polar mutations on the protein surface should increase the stability of the protein. We chose the hydrophobic residues that are exposed to solvent and adjacent to the N-glycosylation sites in the modeled structure of IL5R $\alpha$ <sup>12</sup> and generated double or triple mutations in those regions based on sequence alignment with mouse IL5R $\alpha$ , human prolactin receptor, and human growth hormone receptor (Figure 1). The extracellular domains of prolactin and growth hormone receptors were produced in *Escherichia coli*, and their crystal structures in complex with their ligand have been determined,<sup>29,30</sup> indicating the structural stability of the deglycosylated forms. We found that mutants such as I109V/V110T/N111Q, I109V/V110T/N111D, and L223R/

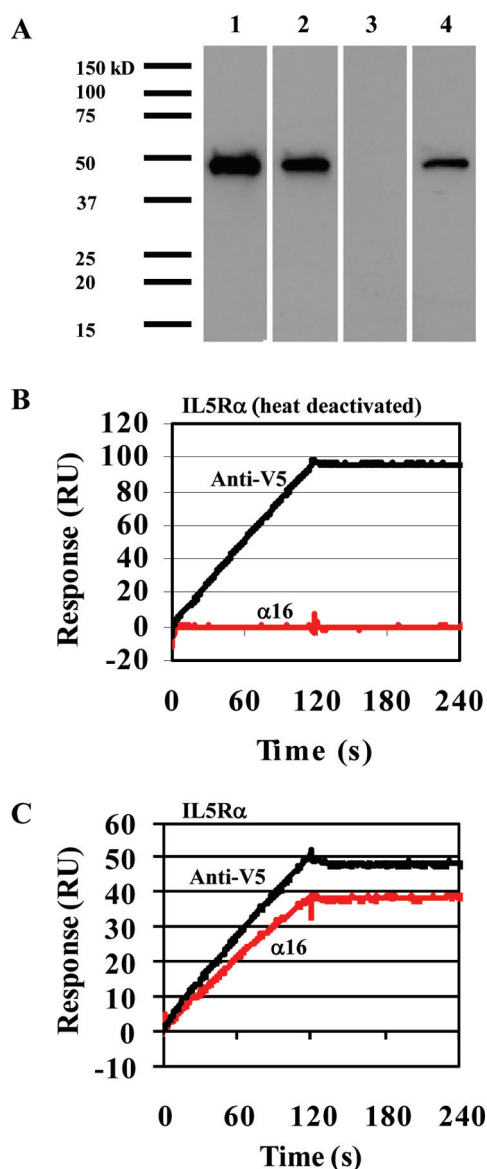


**Figure 2.** Characterization of a conformationally sensitive anti-IL5R $\alpha$  antibody. (A) Western blotting of the expressed soluble domain of IL5R $\alpha$ . The conditioned medium containing soluble IL5R $\alpha$  was mixed with SDS buffer, boiled for 10 min, and loaded onto an SDS-PAGE gel: lane 1, band stained with anti-IL5R $\alpha$  mAb (R&D Systems); lane 2, anti-V5-tag pAb (Invitrogen); lane 3, anti-IL5R $\alpha$  mAb  $\alpha$ 16; lane 4, anti-IL5R $\alpha$  mAb 2B6R. (B and C) Injection of the heat-deactivated form of purified IL5R $\alpha$  (B) or the native form of purified IL5R $\alpha$  (C) at 0 s, followed by injection of running buffer at 120 s. In this assay, either form of IL5R $\alpha$  protein was injected over the antibody surfaces, and binding of IL5R $\alpha$  to each antibody was monitored. Black lines show the sensorgrams for anti-V5-tag pAb and red lines those for  $\alpha$ 16.

N224Q had almost the same stability as the fully glycosylated form (Figure 3C).

**Ligand Binding Activities of Deglycosylated Mutants.** For the ligand binding assay, we chose the most stable deglycosylated mutants at each site. These were N15D (denoted IL5R $\alpha$ [\Delta N15]), I109V/V110T/N111D (denoted IL5R $\alpha$ [\Delta N111]), N196T (denoted IL5R $\alpha$ [\Delta N196]), and L223R/N224Q (denoted IL5R $\alpha$ [\Delta N224]). To validate the kinetic interaction with IL5, we employed a previously established SPR biosensor assay.<sup>12</sup> Briefly, different concen-

trations of IL5 were injected over the IL5R $\alpha$  variants that had been precaptured via their C-terminal V5-tag by the anti-V5-tag antibody immobilized covalently on the biosensor surface (Figure 4). Kinetic analysis showed that deglycosylation variants such as IL5R $\alpha$ [\Delta N15], IL5R $\alpha$ [\Delta N111], and IL5R $\alpha$ [\Delta N224] had almost the same kinetic profiles as fully glycosylated IL5R $\alpha$ , whereas IL5R $\alpha$ [\Delta N196] showed a 5-fold increase in its  $K_d$  value because of the combination of a decreased  $k_{on}$  and an increased  $k_{off}$  (Table 1). Our attempt to obtain a completely deglycosylated IL5R $\alpha$  by using these four mutations resulted in the complete loss of ligand binding and  $\alpha$ 16 binding (data not shown). Because the N196T mutation is most likely the mutation that destabilized the structure of IL5R $\alpha$  (Figure 3), we performed triple-mutational deglycosylation with N15D, I109V/V110T/N111D, and L223R/N224Q but maintained Asn<sup>196</sup> glycosylation to obtain the mostly deglycosylated form of IL5R $\alpha$ . This variant, which had three of four glycosylation sites eliminated (denoted IL5R $\alpha$ [\Delta N15/111/224]), showed the same ligand binding affinity and kinetic parameters as fully glycosylated IL5R $\alpha$  (Figure 4 and Table 1).

**Effect of Lectin on the IL5–IL5R $\alpha$  Interaction.** We conducted further biochemical characterizations of purified IL5R $\alpha$ [\Delta N15/111/224] to elucidate the functional role of the carbohydrate moiety at Asn<sup>196</sup>. MALDI-MS analysis of purified IL5R $\alpha$  showed that the mass of total carbohydrates was 5873 Da, that is, 14% of the total mass of IL5R $\alpha$  (Table 2). On the other hand, the mass of total carbohydrates of IL5R $\alpha$ [\Delta N15/111/224] was 2344 Da, that is, 6% of the total mass of IL5R $\alpha$ [\Delta N15/111/224]. These results indicate that a single carbohydrate moiety at Asn<sup>196</sup> occupies as much as 40% of the total carbohydrate content of IL5R $\alpha$ . To examine the glycosylation at Asn<sup>196</sup>, we characterized the lectin binding activity of IL5R $\alpha$ [\Delta N15/111/224] using an SPR biosensor. In this assay, either concanavalin A (ConA) or cyanovirin-N (CV-N) was immobilized on the biosensor surface, and then either purified IL5R $\alpha$ [\Delta N15/111/224] or purified IL5R $\alpha$  was injected over the lectin surface. We found that the lectin binding affinity of IL5R $\alpha$ [\Delta N15/111/224] was lower than that of fully glycosylated IL5R $\alpha$  (Figure S1 of the Supporting Information), probably because of the reduced carbohydrate content of IL5R $\alpha$ [\Delta N15/111/224]. Because CV-N selectively binds to high-mannose oligosaccharides, the carbohydrate moiety at Asn<sup>196</sup> might be high-mannose, which is consistent with the previous observations on the carbohydrate structure of IL5R $\alpha$ .<sup>13</sup>

To test whether the carbohydrate at Asn<sup>196</sup> is involved in the IL5–IL5R $\alpha$  interaction, we examined binding of IL5 to IL5R $\alpha$ [\Delta N15/111/224] in the presence of CV-N. In this assay, purified IL5R $\alpha$ [\Delta N15/111/224] was captured by CV-N immobilized on the biosensor surface and then nonglycosylated IL5 was injected over the receptor surface. We found that IL5R $\alpha$ [\Delta N15/111/224] binds IL5 with high affinity even when the single carbohydrate group at Asn<sup>196</sup> is occupied by binding to CV-N (Figure S2 of the Supporting Information). This IL5 binding activity suggests that the carbohydrate at Asn<sup>196</sup> of IL5R $\alpha$  is not involved in a direct contact with IL5.

**Biological Activity and Cell Surface Expression.** We asked whether N-glycosylation plays a role in the cellular function of IL5R $\alpha$ . Plasmids encoding the full length of the two deglycosylated variants (IL5R $\alpha$ [\Delta N196] and IL5R $\alpha$ [\Delta N15/111/224]) as well as wild-type IL5R $\alpha$  were stably transfected into BaF3 cells, and IL5-induced cell proliferation in these cells

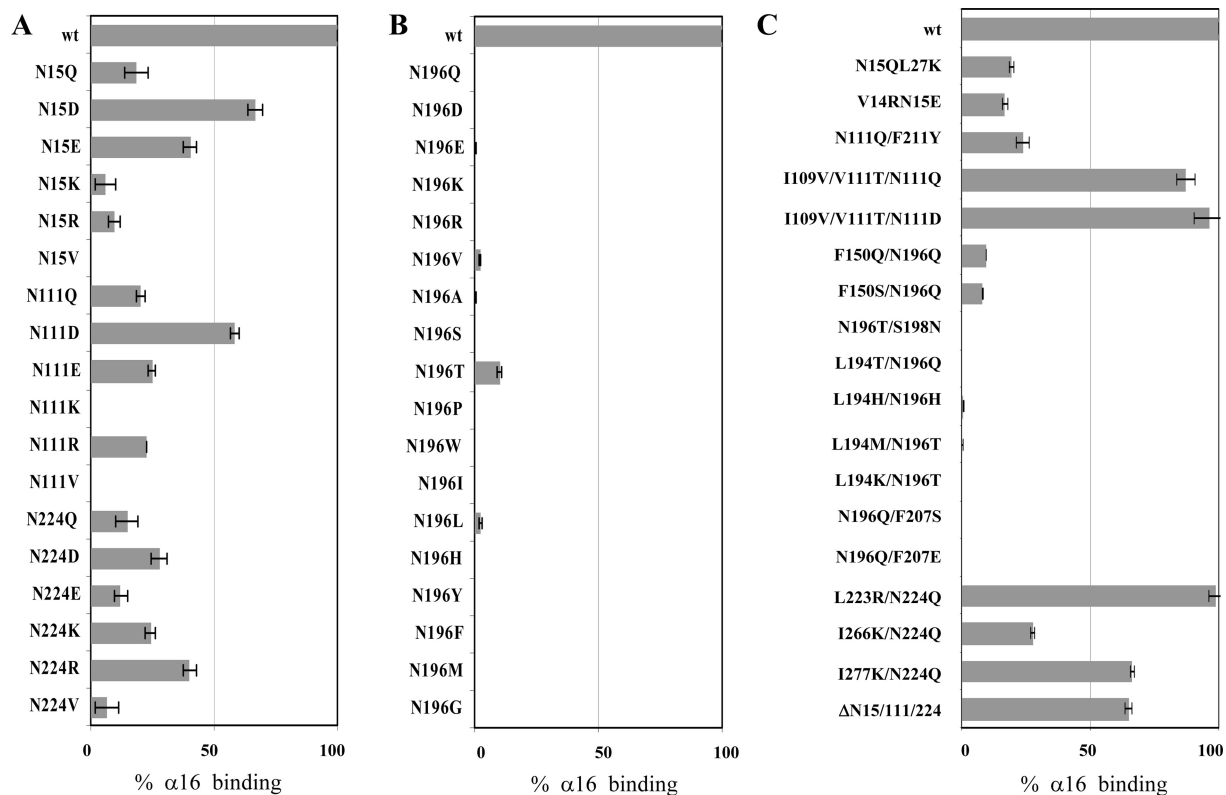


**Figure 3.** Screening assay of the structural integrity of soluble forms of deglycosylation mutants. In this assay, culture supernatant containing IL5R $\alpha$  mutational variants was injected over the immobilized antibody  $\alpha$ 16 SPR chip surface. This antibody surface was used to examine the stability of transiently expressed proteins, while the anti-V5-tag antibody was used to normalize the expression level of the protein. Thus, the ratio of  $\alpha$ 16 binding activity to anti-V5 activity denotes the extent of conformational intactness of the expressed proteins. The percent  $\alpha$ 16 binding level was calculated by dividing amounts of  $\alpha$ 16-binding proteins by those of anti-V5-tag antibody and then by dividing the resulting values of mutants by that of wild-type IL5R $\alpha$ . Individual values were obtained from three experiments. The average values are shown as bars, and standard deviations are shown as lines.

was investigated. BaF3 is an IL3-dependent mouse pro B cell line that intrinsically expresses the  $\beta$ c receptor subunit. Because human IL5 and IL5R $\alpha$  can cross-react with mouse  $\beta$ c, this cell line has been used for the functional analyses of IL5R $\alpha$  mutational variants.<sup>25</sup> Cells transfected with full-length IL5R $\alpha$  [ $\Delta$ N15/111/224] exhibited IL5-induced cell proliferation similar to that found with fully glycosylated IL5R $\alpha$  (Figure 5), indicating that N-glycosylations at Asn<sup>15</sup>, Asn<sup>111</sup>, and Asn<sup>222</sup> of IL5R $\alpha$  are not important for the cell proliferation activity of the receptor. On the other hand, cells transfected with full-length IL5R $\alpha$  [ $\Delta$ N196] exhibited no proliferation (Figure 5A). To determine whether the N196T mutation completely suppressed the biological function because of the absence of the receptor on the cell surface, we assessed the cell surface expression of the deglycosylated mutant with anti-IL5R $\alpha$  antibodies. Flow cytometry analysis revealed no signal shift in BaF3 cells transfected with full-length IL5R $\alpha$  [ $\Delta$ N196], whereas signal shifts were detected in BaF3 cells transfected with either fully glycosylated IL5R $\alpha$  or IL5R $\alpha$  [ $\Delta$ N15/111/224] (Figure 5B). These data indicate that IL5R $\alpha$  [ $\Delta$ N196] was not expressed on the cell. Hence, N-glycosylation at Asn<sup>196</sup> might be required for transport of IL5R $\alpha$  to the cell surface.

## DISCUSSION

We have previously shown the effects of amino acid replacement of human IL5R $\alpha$  on ligand binding and receptor antagonism.<sup>12,31,32</sup> The main purpose of this study was to

provide insights into the specific roles of N-glycosylation of IL5R $\alpha$  in its structure and function. IL5R $\alpha$  contains four consensus N-glycosylation sites (Asn-X-Ser/Thr) at Asn<sup>15</sup>, Asn<sup>111</sup>, Asn<sup>196</sup>, and Asn<sup>224</sup> in the extracellular region (Figure 1). In general, N-glycosylation of proteins can play an important role in a variety of aspects, such as ligand binding, protein folding, trafficking, and stability.<sup>14–16,33,34</sup> We have previously found that enzymatic deglycosylation of IL5R $\alpha$  weakened its ability to bind IL5.<sup>13</sup> However, it has remained unclear whether all of the N-glycosylations are involved in ligand binding or if only a specific subset of N-glycosylation sites is necessary. It also was unclear what caused such a drastic loss of ligand binding. To answer these questions, we investigated the structural and functional roles of N-glycosylation sites by site-directed mutagenesis. We initially introduced an Asn-to-Gln mutation as one of the general approaches to mutational deglycosylation. However, we found that such a mutation caused significant decreases in the level of protein expression (data not shown) as well as losses of binding to its conformationally sensitive antibody (Figure 3), suggesting that introduction of glutamine at these points destabilizes the structure of IL5R $\alpha$ . Therefore, we evaluated the ability of a series of combinatorial and rationally designed mutations to preserve the stability of deglycosylated mutants of IL5R $\alpha$ . The former approach is based on a hypothesis that asparagine residues at the N-glycosylation sites can be replaced with certain charged residues while maintaining the stability of the protein.<sup>18</sup> The latter approach is based on a finding that the

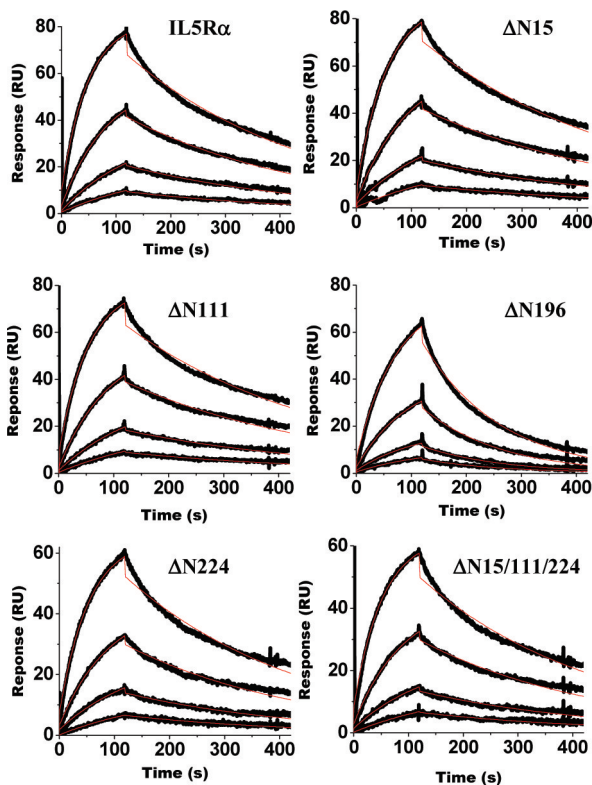


**Figure 4.** Ligand binding of deglycosylated variants. The soluble forms of wild-type ILSRα and five deglycosylation mutants were transiently expressed in S2 cells, and the supernatants were injected over the anti-V5-tag antibody biosensor chip surface on the biosensor (“on-chip purification”). Subsequently, various concentrations (5, 10, 20, and 40 nM) of IL5 were injected at 0 s, followed by injection of running buffer alone at 120 s. The rate constants were calculated by globally fitting the association phase (0–120 s) and the dissociation phase (120–360 s) to a model for 1:1 Langmuir binding. Red lines show calculated sensorgrams. Individual kinetic parameters were obtained from three separate experiments. The average and standard deviation are listed in Table 1.

stability and solubility of glycan-free forms of glycoproteins can be improved by using apolar-to-polar mutations of any surface residue in functionally irrelevant epitopes.<sup>17</sup> We utilized a conformationally sensitive anti-ILSRα mAb as a marker to verify the structural integrity of ILSRα and performed a medium-throughput assay of all the deglycosylated mutants with a surface plasmon resonance (SPR) biosensor (Figure 2).

From these two protein engineering approaches, we generated a total of 54 deglycosylation mutations (Figure 3). We found that mutations such as N15D, N111D, and N224R displayed significantly increased structural stability relative to the Asn-to-Gln mutation, while any replacement at Asn<sup>196</sup>

**Table 2.** Comparison of Carbohydrate Contents of Wild-Type and Mostly Deglycosylated ILSRα Determined by MALDI-TOF MS

	MS(calc)	MS(exp)	ΔMS(exp–calc)	ΔMS(wt mutant)
ILSRα	35877	41750	5873	–
ILSRα[ΔN15/111/224]	36447	38791	2344	3529

severely reduced stability (Figure 3A,B). Interestingly, Asn-to-Asp mutations were more stable than Asn-to-Glu or Asn-to-Gln mutations at Asn<sup>15</sup>, Asn<sup>111</sup>, and Asn<sup>224</sup>, suggesting that not only the charge of an amino acid but also its molecular volume might be important for the stability of local structure. These data imply that the Asn-to-Gln mutation, which is generally chosen for deglycosylation because of the retention of electrostatic properties, may not be the best strategy for all glycoproteins. Although any replacement at Asn<sup>196</sup> with charged residues severely reduced stability, substitution with threonine gave the best result (Figure 3B). It should be noted that threonine is the residue at the corresponding position of the human prolactin receptor in our sequence alignment (Figure 1). From rationally designed mutations, we found that ILSRα[ΔN111] (I109V/V110T/N111D) and ILSRα[ΔN224] (L223R/N224Q) had almost the same structural stability as the fully glycosylated form of ILSRα (Figure 3C).

Because ILSRα[ΔN15], ILSRα[ΔN111], and ILSRα[ΔN224] mutants have almost the same stability and binding affinity for IL5 (Figure 4 and Table 1), we engineered a deglycosylated variant from which three of four glycosylation sites have been eliminated. This mostly deglycosylated variant (denoted ILSRα[ΔN15/111/224]) also exhibited the same binding affinity for IL5 as fully glycosylated ILSRα. We sought a rationale for these stability-preserving mutations in a homology-modeled structure of ILSRα[ΔN15/111/224]. We found that mutations such as N15D and L223R/N224Q might stabilize the structure through interactions with neighboring charged residues. In the model, the side chain of Asp<sup>15</sup> appears to interact with the side chain of Lys<sup>19</sup> (Figure 6A), and therefore, the Asn-to-Gln mutation at this position would be expected to lead to a loss of a favorable charge interaction. The side chains of Arg<sup>223</sup> and Gln<sup>224</sup> appear to stabilize the interstrand conformation by interacting with the side chain of Glu<sup>239</sup> in the neighboring strand (Figure 6B). In contrast, no favorable interactions of mutated residues in the N111 region (I109V/V110T/N111Q) were observed with neighboring residues in the modeled structure, even though the I109V/V110T/N111Q mutant preserved the stability to the same extent as fully glycosylated ILSRα. Perhaps the combination of apolar and polar groups in this locus is sufficient to contribute entropically to the stabilization of the protein. One could imagine that Asn-to-Gln mutation alone at positions 111 and

**Table 1.** Kinetic Interaction between IL5 and Soluble Forms of ILSRα Deglycosylated Variants

mutations		$k_{on}$ ( $\times 10^{-6}$ M <sup>-1</sup> s <sup>-1</sup> )	$k_{off}$ ( $\times 10^3$ s <sup>-1</sup> )	$K_d$ ( $\times 10^9$ M)
wild-type ILSRα		1.2 ± 0.3	3.1 ± 0.1	2.7 ± 0.1
ILSRα[ΔN15]	N15D	1.0 ± 0.8	2.5 ± 0.1	2.5 ± 0.2
ILSRα[ΔN111]	I109V/V110T/N111D	1.1 ± 0.7	3.0 ± 0.2	2.7 ± 0.1
ILSRα[ΔN196]	N196T	0.47 ± 0.3	7.1 ± 0.1	15 ± 1
ILSRα[ΔN224]	L223R/N224Q	1.0 ± 0.4	3.3 ± 0.2	3.3 ± 0.1
ILSRα[ΔN15/111/224]	N15D, I109V/V110T/N111D, and L223R/N224Q	1.0 ± 0.3	3.4 ± 0.2	3.2 ± 0.2

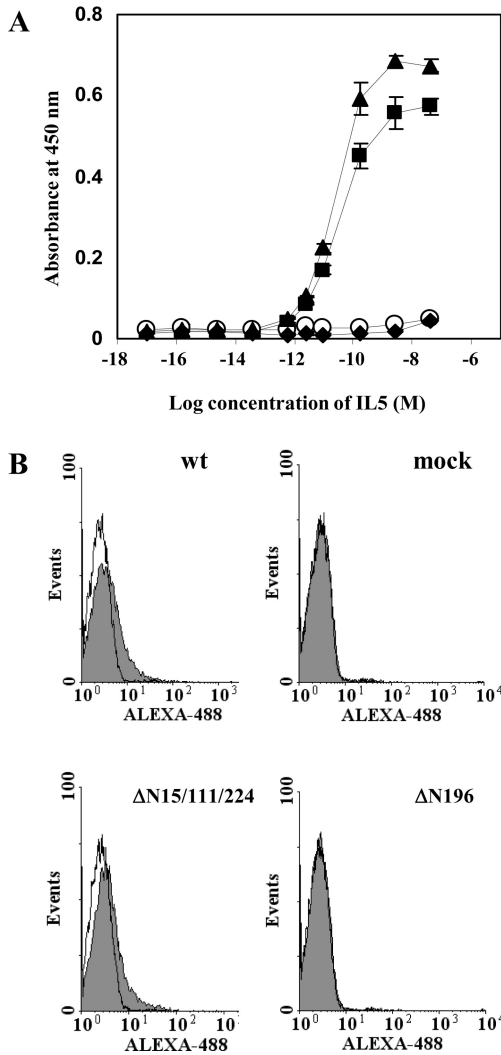


**Figure 5.** Cell proliferation activity and cell surface expression of full-length IL5R $\alpha$  deglycosylation mutants. (A) The IL3-dependent mouse BaF3 cell line was used to test the bioactivity of exogenously expressed full-length IL5R $\alpha$  (▲), full-length IL5R $\alpha$ [ $\Delta$ N15/111/224] (■), full-length IL5R $\alpha$ [ $\Delta$ N196] (◆), and empty vector (○). Five thousand cells per well were incubated with various dilutions (0.01 fM to 40 nM) of IL5. After incubation for 48 h, proliferation was evaluated as described in Experimental Procedures. The average values of triplicate wells are plotted with standard deviations. (B) Cytofluorometric analysis of cellular surface expression of the wild type and mutant of full-length IL5R $\alpha$  on BaF3 transfectants. Cells were incubated with anti-IL5R $\alpha$  antibodies or negative control (17b) as the primary antibody and Alexa-conjugated goat anti-mouse pAb (Invitrogen) as the secondary antibody. Histogram plots from 2B6R (gray area) show the expression of full-length forms of wild-type IL5R $\alpha$  (wt) and IL5R $\alpha$ [ $\Delta$ N15/111/224] ( $\Delta$ N15/111/224) compared to no expression of empty vector (mock) and IL5R $\alpha$ [ $\Delta$ N196] ( $\Delta$ N196). The negative control indicates staining with the secondary antibody alone (black lines).

224 might not be sufficient to stabilize the local conformation without other favorable interactions or increased hydrophilicity at nearby mutational sites. In any case, the model suggests that some carbohydrate moieties of IL5R $\alpha$  could be replaced without compromising the stability and function of IL5R $\alpha$  protein.

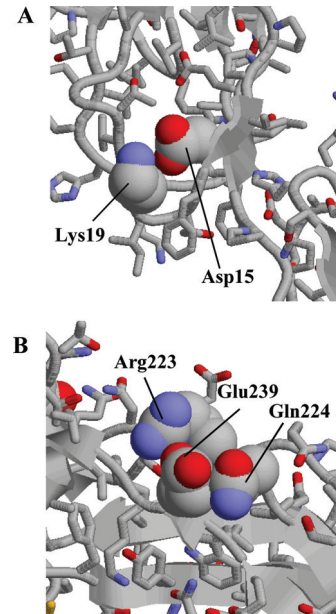


**Figure 6.** Potential charged interactions and hydrogen bonds introduced by the mutations at N-glycosylation sites. The homology-modeled structure of IL5R $\alpha$ [ $\Delta$ N15/111/224], based on a previously reported model of IL5R $\alpha$ , suggests potential favorable interactions upon deglycosylation mutation at Asn<sup>15</sup> (A) and Asn<sup>224</sup> (B). The residues of interest are shown as a CPK model. Oxygen and nitrogen atoms are colored red and blue, respectively. All the molecular graphics in this article were prepared with RasMol.<sup>50</sup>

IL5R $\alpha$  is a member of the class I cytokine receptor superfamily, members of which are characterized by the presence of the so-called cytokine recognition motif.<sup>35</sup> Extensive structural studies have been performed for various cytokine–receptor complexes in this superfamily (reviewed in references 36 and 37). In some cases (e.g., G-CSF<sup>38</sup>), crystal structures of the cytokine–receptor complex have been determined without deglycosylation. However, early trials to obtain crystals of the fully glycosylated IL5R $\alpha$  in complex with deglycosylated IL5 proved unsuccessful.<sup>13</sup> Because carbohydrate moieties of glycoproteins affect crystal formation, deglycosylation prior to crystallization could improve the chances for obtaining high-quality crystals. For deglycosylation of the cytokine receptors, the following four methods have been used: bacterial expression (e.g., growth hormone,<sup>29</sup> prolactin,<sup>30</sup> and IL4<sup>39</sup>), enzymatic deglycosylation (e.g., IL10<sup>40</sup> and IL12<sup>41</sup>), mutational deglycosylation (e.g., erythropoietin<sup>42</sup> and IL6<sup>43</sup>), and inhibition of glycosidase (e.g., IL2<sup>44</sup>). Most recently, Hansen et al. have successfully determined the crystal structure of the receptor complex of GM-CSF, which is the closest homologue of IL5, by using GM-CSF from bacterial expression, a fully glycosylated  $\alpha$  subunit, and a  $\beta$ / $\gamma$  subunit with Asn-to-Gln mutational deglycosylation.<sup>45</sup> Here, we utilized site-directed mutagenesis and engineered IL5R $\alpha$ [ $\Delta$ N15/111/224], which retained Asn<sup>196</sup>, while eliminating the other three glycosylation sites of IL5R $\alpha$ . This mostly deglycosylated variant might facilitate crystallization of the IL5–receptor complex, and the stability-preserving deglycosylation strategies presented here could be applied to crystallographic analyses of other glycoproteins.

Our data demonstrated that deglycosylation at Asn<sup>196</sup> of IL5R $\alpha$  severely reduced its stability and binding affinity for IL5



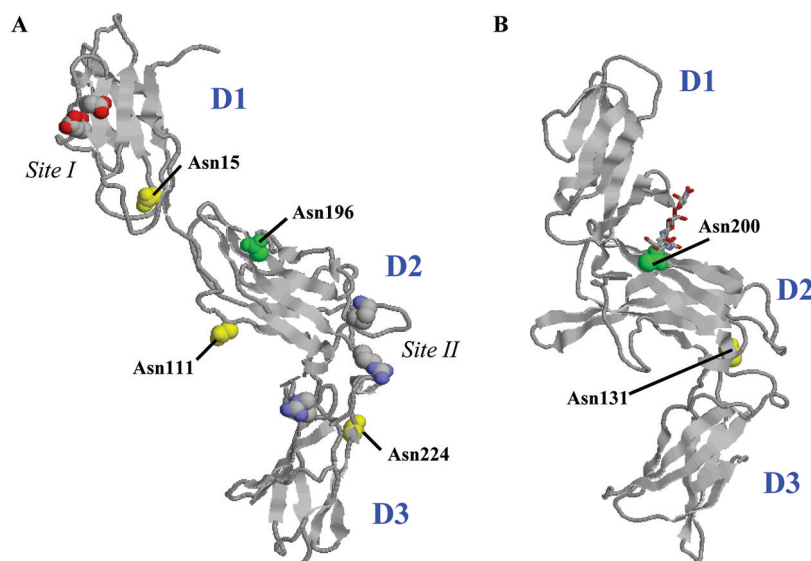


**Figure 7.** Maps of the N-glycosylation sites and ligand binding epitopes on the homology-modeled structure of IL5R $\alpha$  compared with the crystal structure of IL12. (A) Modeled structure of IL5R $\alpha$ .<sup>12</sup> (B) Crystal structure of IL12 p40.<sup>41</sup> Three fibronectin type III domains (D1, D2, and D3) are denoted from the N- to C-terminus. Asn<sup>196</sup> of IL5R $\alpha$  and Asn<sup>200</sup> of IL12 are colored green, and other asparagine residues for N-glycosylation are colored yellow. The IL5-binding residues at site I and II epitopes, which have been found previously,<sup>12,52</sup> are shown as a CPK model. The loop regions are represented as coils and  $\beta$  strands as ribbons. Carbohydrate groups are shown as stick models. GlcNAc and Man stand for *N*-acetylglucosamine and mannose, respectively.

(Figure 3 and Figure 4). We also observed that IL5R $\alpha$ [\Delta N196] lost ligand binding activity over time (data not shown). These findings inspired us to test whether deglycosylation at Asn<sup>196</sup> of IL5R $\alpha$  caused a reduction in the ligand binding activity not because the carbohydrate is involved in the direct interaction with the ligand but as a secondary effect of the partially destabilized structure of IL5R $\alpha$  upon deglycosylation. We have previously shown that IL5-binding residues are located in the D1 domain (Asp<sup>55</sup>, Asp<sup>56</sup>, and Glu<sup>58</sup>) as well as in the D2 domain (Lys<sup>186</sup> and Arg<sup>188</sup>) and the D3 domain (Arg<sup>297</sup>).<sup>12</sup> The binding interface of IL5R $\alpha$  comprises a cluster of negatively charged residues [site I epitope (Figure 7A)] from the D1 domain and a cluster of positively charged residues [site II epitope (Figure 7A)] from the D2D3 tandem domain. The homology-deduced IL5R $\alpha$  structure shows that Asn<sup>196</sup> in the D2 domain is not located in the proximity of either site I or II epitopes (Figure 7A). The four N-glycosylation sites of IL5R $\alpha$  are conserved in GM-CSF receptor  $\alpha$ , which shares a high degree of amino acid sequence similarity with IL5R $\alpha$  as well as signaling receptor  $\beta$ c (sequence alignment available in reference 32). The crystal structure of the GM-CSF receptor complex showed no direct interaction of the receptor carbohydrate and ligand.<sup>45</sup> Moreover, our lectin inhibition assay showed that neither cyanovirin-N nor concanavalin-A had any impact on the interaction of IL5R $\alpha$ [\Delta N15/111/224] with deglycosylated IL5 (Figure S2 of the Supporting Information). From these observations, we conclude that the carbohydrate at Asn<sup>196</sup> is less likely involved in the direct interaction between IL5 and IL5R $\alpha$  and instead likely plays a critical role in maintaining the correct structure of the receptor. Interestingly, Yoon et al.<sup>41</sup> found that a carbohydrate extending from Asn<sup>200</sup> of the D2 domain lies in the interface of the D1 and D2 domains in the crystal structure of the p35–p40 heterodimer of IL12 (Figure 7B). They have proposed that the carbohydrate stabilizes the structure by fixing the relative orientation of these domains through hydrogen bonds and van der Waals contacts. It is

noteworthy that the spatial position of Asn<sup>196</sup> of IL5R $\alpha$  is similar to that of Asn<sup>200</sup> of IL12 (Figure 7). Although the detailed structural role of the carbohydrate at Asn<sup>196</sup> of IL5R $\alpha$  must await high-resolution structure determination of the IL5–IL5R $\alpha$ [\Delta N15/111/224] complex by X-ray crystallography, it is tempting to speculate that the carbohydrate at Asn<sup>196</sup> might stabilize the overall structure of the receptor by bridging the D1 and D2 domains as in the IL12 system.

We developed a medium-throughput screening assay to characterize the structural integrity and ligand binding affinity of the extracellular domain of IL5R $\alpha$  by using the transient expression system with *Drosophila* S2 insect cells. Although insect expression facilitates overexpression and screening of a large number of recombinant proteins, it is known that the carbohydrate components of N-glycosylation of insect cells are different from those of mammalian cells.<sup>46,47</sup> To verify the role of N-glycosylation of IL5R $\alpha$  in mammalian cells, we used the BaF3 cell line, a mouse pro B cell line that has been used for functional analyses of human IL5R $\alpha$ .<sup>25,48</sup> Using BaF3 cells expressing full-length IL5R $\alpha$  and its mutational variants, we found that deglycosylation at Asn<sup>196</sup> resulted in the failure of cell surface expression of IL5R $\alpha$  (Figure 5B) and caused a complete loss of the biological response to IL5 (Figure 5A). In light of the finding that the carbohydrate at Asn<sup>196</sup> is likely indispensable for the correct structure of the receptor (see above), it is plausible that Asn<sup>196</sup> deglycosylation causes the failure of cell surface expression of IL5R $\alpha$ [\Delta N196] by destabilizing the structure of IL5R $\alpha$ .

In conclusion, this study reveals the essential role of a single carbohydrate moiety at Asn<sup>196</sup> in the structure and function of IL5R $\alpha$ . Our unique protein engineering approach also demonstrated that most, but not all, N-linked carbohydrates can be eliminated without compromising the function of the protein via introduction of targeted mutations at and around N-glycosylation sites. We obtained a stable and functional variant that has three of four glycosylation sites eliminated. The mostly

deglycosylated form we obtained in this study could open the way to improving high-resolution structural analysis of the IL5 system and help in the design of new compounds for therapeutic treatment of IL5-related allergic inflammatory diseases.

## ■ ASSOCIATED CONTENT

### ● Supporting Information

Biosensor data of kinetic interaction of lectin and IL5R $\alpha$  deglycosylation variants. This material is available free of charge via the Internet at <http://pubs.acs.org>.

## ■ AUTHOR INFORMATION

### Corresponding Author

\*E-mail: [Irwin.Chaiken@DrexelMed.edu](mailto:Irwin.Chaiken@DrexelMed.edu). Phone: (215) 762-4197. Fax: (215) 762-4452.

### Present Address

<sup>1</sup>Pfizer Global Research & Development, 87 Cambridgepark Dr., Cambridge, MA 02140.

### Funding

This work was supported by National Institutes of Health Grant AI40462.

## ■ ACKNOWLEDGMENTS

We thank Dr. Keith A. Vosseller (Drexel University College of Medicine) for the useful discussion.

## ■ ABBREVIATIONS

IL5R $\alpha$ , human interleukin-5 receptor  $\alpha$ ; GM-CSF, granulocyte/macrophage colony-stimulating factor; PBS, phosphate-buffered saline; SPR, surface plasmon resonance; RU, resonance unit; GFP, green fluorescent protein; ConA, concanavalin A; CV-N, cyanovirin-N; mAb, monoclonal antibody; pAb, polyclonal antibody;  $\Delta$ N15, N15D mutant of IL5R $\alpha$ ;  $\Delta$ N111, I109V/V110T/N111D mutant of IL5R $\alpha$ ;  $\Delta$ N196, N196T mutant of IL5R $\alpha$ ;  $\Delta$ N224, L223R/N224Q mutant of IL5R $\alpha$ ;  $\Delta$ N15/111/224, N15/I109V/V110T/N111D/L223R/N224Q mutant of IL5R $\alpha$ .

## ■ REFERENCES

- (1) Karlen, S., De Boer, M. L., Lipscombe, R. J., Lutz, W., Mordvinov, V. A., and Sanderson, C. J. (1998) Biological and molecular characteristics of interleukin-5 and its receptor. *Int. Rev. Immunol.* *16*, 227–247.
- (2) Sanderson, C. J., and Urwin, D. (2000) Interleukin-5: A drug target for allergic diseases. *Curr. Opin. Invest. Drugs* *1*, 435–441.
- (3) Foster, P. S., Hogan, S. P., Yang, M., Mattes, J., Young, I. G., Matthaei, K. I., Kumar, R. K., Mahalingam, S., and Webb, D. C. (2002) Interleukin-5 and eosinophils as therapeutic targets for asthma. *Trends Mol. Med.* *8*, 162–167.
- (4) Rothenberg, M. E. (2004) Eosinophilic gastrointestinal disorders (EGID). *J. Allergy Clin. Immunol.* *113*, 11–28.
- (5) Zaks-Zilberman, M., Harrington, A. E., Ishino, T., and Chaiken, I. M. (2008) Interleukin-5 receptor subunit oligomerization and rearrangement revealed by fluorescence resonance energy transfer imaging. *J. Biol. Chem.* *283*, 13398–13406.
- (6) Ishino, T., Harrington, A. E., Zaks-Zilberman, M., Scibek, J. J., and Chaiken, I. (2008) Slow-dissociation effect of common signaling subunit  $\beta$ c on IL5 and GM-CSF receptor assembly. *Cytokine* *42*, 179–190.
- (7) Scibek, J. J., Evergren, E., Zahn, S., Canziani, G. A., Van Ryk, D., and Chaiken, I. M. (2002) Biosensor analysis of dynamics of

interleukin 5 receptor subunit  $\beta$ c interaction with IL5:IL5R $\alpha$  complexes. *Anal. Biochem.* *307*, 258–265.

(8) Carr, P. D., Gustin, S. E., Church, A. P., Murphy, J. M., Ford, S. C., Mann, D. A., Woltring, D. M., Walker, I., Ollis, D. L., and Young, I. G. (2001) Structure of the complete extracellular domain of the common  $\beta$  subunit of the human GM-CSF, IL-3, and IL-5 receptors reveals a novel dimer configuration. *Cell* *104*, 291–300.

(9) Morton, T., Li, J., Cook, R., and Chaiken, I. (1995) Mutagenesis in the C-terminal region of human interleukin 5 reveals a central patch for receptor  $\alpha$  chain recognition. *Proc. Natl. Acad. Sci. U.S.A.* *92*, 10879–10883.

(10) Tavernier, J., Tuypens, T., Verhee, A., Plaetinck, G., Devos, R., Van der Heyden, J., Guisez, Y., and Oefner, C. (1995) Identification of receptor-binding domains on human interleukin 5 and design of an interleukin 5-derived receptor antagonist. *Proc. Natl. Acad. Sci. U.S.A.* *92*, 5194–5198.

(11) Cornelis, S., Plaetinck, G., Devos, R., Van der Heyden, J., Tavernier, J., Sanderson, C. J., Guisez, Y., and Fiers, W. (1995) Detailed analysis of the IL-5-IL-5R $\alpha$  interaction: Characterization of crucial residues on the ligand and the receptor. *EMBO J.* *14*, 3395–3402.

(12) Ishino, T., Pasut, G., Scibek, J., and Chaiken, I. (2004) Kinetic interaction analysis of human interleukin 5 receptor  $\alpha$  mutants reveals a unique binding topology and charge distribution for cytokine recognition. *J. Biol. Chem.* *279*, 9547–9556.

(13) Johanson, K., Appelbaum, E., Doyle, M., Hensley, P., Zhao, B., Abdel-Meguid, S. S., Young, P., Cook, R., Carr, S., Matico, R., et al. (1995) Binding interactions of human interleukin 5 with its receptor  $\alpha$  subunit. Large scale production, structural, and functional studies of *Drosophila*-expressed recombinant proteins. *J. Biol. Chem.* *270*, 9459–9471.

(14) West, C. M. (1986) Current ideas on the significance of protein glycosylation. *Mol. Cell. Biochem.* *72*, 3–20.

(15) Helenius, A. (1994) How N-linked oligosaccharides affect glycoprotein folding in the endoplasmic reticulum. *Mol. Biol. Cell* *5*, 253–265.

(16) Niu, L., Heaney, M. L., Vera, J. C., and Golde, D. W. (2000) High-affinity binding to the GM-CSF receptor requires intact N-glycosylation sites in the extracellular domain of the  $\beta$  subunit. *Blood* *95*, 3357–3362.

(17) Sun, Z. Y., Dotsch, V., Kim, M., Li, J., Reinherz, E. L., and Wagner, G. (1999) Functional glycan-free adhesion domain of human cell surface receptor CD58: Design, production and NMR studies. *EMBO J.* *18*, 2941–2949.

(18) Narhi, L. O., Arakawa, T., Aoki, K., Wen, J., Elliott, S., Boone, T., and Cheetham, J. (2001) Asn to Lys mutations at three sites which are N-glycosylated in the mammalian protein decrease the aggregation of *Escherichia coli*-derived erythropoietin. *Protein Eng.* *14*, 135–140.

(19) Wu, S. J., Tambyraja, R., Zhang, W., Zahn, S., Godillot, A. P., and Chaiken, I. (2000) Epitope randomization redefines the functional role of glutamic acid 110 in interleukin-5 receptor activation. *J. Biol. Chem.* *275*, 7351–7358.

(20) McFadden, K., Cocklin, S., Gopi, H., Baxter, S., Ajith, S., Mahmood, N., Shattock, R., and Chaiken, I. (2007) A recombinant allosteric lectin antagonist of HIV-1 envelope gp120 interactions. *Proteins* *67*, 617–629.

(21) Tavernier, J., Van der Heyden, J., Verhee, A., Brusselle, G., Van Ostade, X., Vandekerckhove, J., North, J., Rankin, S. M., Kay, A. B., and Robinson, D. S. (2000) Interleukin 5 regulates the isoform expression of its own receptor  $\alpha$ -subunit. *Blood* *95*, 1600–1607.

(22) Pace, C. N., Vajdos, F., Fee, L., Grimsley, G., and Gray, T. (1995) How to measure and predict the molar absorption coefficient of a protein. *Protein Sci.* *4*, 2411–2423.

(23) Dowd, C. S., Leavitt, S., Babcock, G., Godillot, A. P., Van Ryk, D., Canziani, G. A., Sodroski, J., Freire, E., and Chaiken, I. M. (2002)  $\beta$ -turn Phe in HIV-1 Env binding site of CD4 and CD4 mimetic

miniprotein enhances Env binding affinity but is not required for activation of co-receptor/17b site. *Biochemistry* 41, 7038–7046.

(24) Myszka, D. G. (2000) Kinetic, equilibrium, and thermodynamic analysis of macromolecular interactions with BIACORE. *Methods Enzymol.* 323, 325–340.

(25) Cornelis, S., Fache, I., Van derHeyden, J., Guisez, Y., Tavernier, J., Devos, R., Fiers, W., and Plaetinck, G. (1995) Characterization of critical residues in the cytoplasmic domain of the human interleukin-5 receptor  $\alpha$  chain required for growth signal transduction. *Eur. J. Immunol.* 25, 1857–1864.

(26) Sali, A., and Blundell, T. L. (1993) Comparative protein modelling by satisfaction of spatial restraints. *J. Mol. Biol.* 234, 779–815.

(27) Laskowski, R., MacArthur, M., Moss, D., and Thornton, J. (1993) PROCHECK: A program to check the stereochemical quality of protein structures. *J. Appl. Crystallogr.* 26, 283–291.

(28) Sippl, M. J. (1993) Recognition of errors in three-dimensional structures of proteins. *Proteins* 17, 355–362.

(29) de Vos, A. M., Ultsch, M., and Kossiakoff, A. A. (1992) Human growth hormone and extracellular domain of its receptor: Crystal structure of the complex. *Science* 255, 306–312.

(30) Somers, W., Ultsch, M., De Vos, A. M., and Kossiakoff, A. A. (1994) The X-ray structure of a growth hormone-prolactin receptor complex. *Nature* 372, 478–481.

(31) Ishino, T., Pillalamarri, U., Panarello, D., Bhattacharya, M., Urbina, C., Horvat, S., Sarkhel, S., Jameson, B., and Chaiken, I. (2006) Asymmetric usage of antagonist charged residues drives interleukin-5 receptor recruitment but is insufficient for receptor activation. *Biochemistry* 45, 1106–1115.

(32) Ishino, T., Urbina, C., Bhattacharya, M., Panarello, D., and Chaiken, I. (2005) Receptor epitope usage by interleukin 5 mimetic peptide. *J. Biol. Chem.* 280, 22951–22961.

(33) Waetzig, G. H., Chalaris, A., Rosenstiel, P., Suthaus, J., Holland, C., Karl, N., Valles Uriarte, L., Till, A., Scheller, J., Grotzinger, J., Schreiber, S., Rose-John, S., and Seeger, D. (2010) N-linked glycosylation is essential for the stability but not the signaling function of the interleukin-6 signal transducer glycoprotein 130. *J. Biol. Chem.* 285, 1781–1789.

(34) McElroy, C. A., Dohm, J. A., and Walsh, S. T. (2009) Structural and biophysical studies of the human IL-7/IL-7R $\alpha$  complex. *Structure* 17, 54–65.

(35) Taniguchi, T. (1995) Cytokine signaling through nonreceptor protein tyrosine kinases. *Science* 268, 251–255.

(36) Walter, M.R. (2002) Crystal structures of  $\alpha$ -helical cytokine-receptor complexes: We've only scratched the surface. *Biotechniques* 46–48 (Suppl.), 50–47.

(37) Wang, X., Lupardus, P., Laporte, S. L., and Garcia, K. C. (2009) Structural Biology of Shared Cytokine Receptors. *Annu. Rev. Immunol.* 27, 29–60.

(38) Aritomi, M., Kunishima, N., Okamoto, T., Kuroki, R., Ota, Y., and Morikawa, K. (1999) Atomic structure of the GCSF-receptor complex showing a new cytokine-receptor recognition scheme. *Nature* 401, 713–717.

(39) Hage, T., Sebald, W., and Reinemer, P. (1999) Crystal structure of the interleukin-4/receptor  $\alpha$  chain complex reveals a mosaic binding interface. *Cell* 97, 271–281.

(40) Josephson, K., Logsdon, N. J., and Walter, M. R. (2001) Crystal structure of the IL-10/IL-10R1 complex reveals a shared receptor binding site. *Immunity* 15, 35–46.

(41) Yoon, C., Johnston, S. C., Tang, J., Stahl, M., Tobin, J. F., and Somers, W. S. (2000) Charged residues dominate a unique interlocking topography in the heterodimeric cytokine interleukin-12. *EMBO J.* 19, 3530–3541.

(42) Syed, R. S., Reid, S. W., Li, C., Cheetham, J. C., Aoki, K. H., Liu, B., Zhan, H., Osslund, T. D., Chirino, A. J., Zhang, J., Finer-Moore, J.,

Elliott, S., Sitney, K., Katz, B. A., Matthews, D. J., Wendoloski, J. J., Egrie, J., and Stroud, R. M. (1998) Efficiency of signalling through cytokine receptors depends critically on receptor orientation. *Nature* 395, 511–516.

(43) Boulanger, M. J., Chow, D. C., Brevnova, E. E., and Garcia, K. C. (2003) Hexameric structure and assembly of the interleukin-6/IL-6  $\alpha$ -receptor/gp130 complex. *Science* 300, 2101–2104.

(44) Wang, X., Rickert, M., and Garcia, K. C. (2005) Structure of the quaternary complex of interleukin-2 with its  $\alpha$ ,  $\beta$ , and  $\gamma$  receptors. *Science* 310, 1159–1163.

(45) Hansen, G., Hercus, T. R., McClure, B. J., Stomski, F. C., Dottore, M., Powell, J., Ramshaw, H., Woodcock, J. M., Xu, Y., Guthridge, M., McKinstry, W. J., Lopez, A. F., and Parker, M. W. (2008) The structure of the GM-CSF receptor complex reveals a distinct mode of cytokine receptor activation. *Cell* 134, 496–507.

(46) Davidson, D. J., and Castellino, F. J. (1991) Structures of the asparagine-289-linked oligosaccharides assembled on recombinant human plasminogen expressed in a *Mamestra brassicae* cell line (IZD-MBOS03). *Biochemistry* 30, 6689–6696.

(47) Benting, J., Lecat, S., Zacchetti, D., and Simons, K. (2000) Protein expression in *Drosophila* Schneider cells. *Anal. Biochem.* 278, 59–68.

(48) Czabotar, P. E., Holland, J., and Sanderson, C. J. (2000) Identification of regions within the third Fc $\gamma$ III-like domain of the IL-5R $\alpha$  involved in IL-5 interaction. *Cytokine* 12, 867–873.

(49) Thompson, J. D., Higgins, D. G., and Gibson, T. J. (1994) CLUSTAL W: Improving the sensitivity of progressive multiple sequence alignment through sequence weighting, position-specific gap penalties and weight matrix choice. *Nucleic Acids Res.* 22, 4673–4680.

(50) Sayle, R. A., and Milner-White, E. J. (1995) RASMOL: Biomolecular graphics for all. *Trends Biochem. Sci.* 20, 374.